Analyst

Cite this: *Analyst*, 2012, **137**, 5260

www.rsc.org/analyst

PAPER

Tactile multisensing on flexible aluminum nitride

Simona Petroni,*[a] Francesco Guido,[a] Bruno Torre,[b] Andrea Falqui,[b] Maria Teresa Todaro,[c] Roberto Cingolani[b] and Massimo De Vittorio[acd]

Received 25th July 2012, Accepted 12th September 2012
DOI: 10.1039/c2an36015b

The integration of a polycrystalline material such as aluminum nitride (AlN) on a flexible substrate allows the realization of elastic tactile sensors showing both piezoelectricity and significant capacitive variation under normal stress. The application of a normal stress on AlN generates deformation of the flexible substrate on which AlN is grown, which results in strain gradient of the polycrystalline layer. The strain gradient is responsible for an additional polarization described in the literature as the flexoelectric effect, leading to an enhancement of the transduction properties of the material. The flexible AlN is synthesized by sputtering deposition on kapton HN (poly 4,4′-oxydiphenyl pyromellitimide) in a highly oriented crystal structure. High orientation is demonstrated by X-ray diffraction spectra (FWHM = 0.55° of AlN (0002)) and HRTEM. The piezoelectric coefficient d_{33} and stress sensitive capacitance are 4.7 ± 0.5 pm V^{-1} and 4×10^{-3} pF kPa^{-1}, respectively. The parallel plate capacitors realized for tactile sensing present a typical dome shape, very elastic under applied stress and sensitive in the pressure range of interest for robotic applications (10 kPa to 1 MPa). The flexibility of the device finalized for tactile applications is assessed by measuring the sensor capacitance before and after shaping the sensing foil on curved surfaces for 1 hour. Bending does not affect sensor's operation, which exhibits an electrical Q factor as high as 210, regardless of the bending, and a maximum capacitance shift of 0.02%.

Introduction

The development of flexible materials for tactile sensing applications has attracted an increasing interest in robotics, ICT and industrial applications.[1–5] Achieving high spatial resolution and reliability in soft tactile sensors is a high priority in robotic applications for the enhancement of robots' capabilities and their safe interaction with humans,[6] when soft tactile sensors are integrated in artificial skin, and for the discrimination of biological tissues during minimal invasive surgery (MIS),[7,8] when soft tactile sensors are used in medical microrobots.

Among transduction methods, nearly all possible mechanisms such as resistive,[9] capacitive,[10] optical,[11] acoustic,[12] magnetic,[13] electrochemical,[14] electrorheological[15] and piezoelectric[16] methods have been used to develop tactile sensors. However, the most investigated are piezoelectric and capacitive methods that, respectively, allow dynamic and static forces detection. The flexible polymeric materials mainly used for soft piezoelectric and capacitive sensors are PVDF (polyvinylidene fluoride)[17] and dielectric elastomers such as PDMS.[10] PVDF has a high piezoelectric coefficient ($d_{33} = -33$ pC N^{-1}), while PDMS is well known for its biocompatibility and soft lithography process capabilities. Nevertheless, PVDF and PDMS exhibit some drawbacks typical of viscoelastic polymers[18] such as time dependent behaviour with energy losses under loading cycles and significant hysteresis. Another considerable drawback in the context of tactile sensing applications is the cross-talk between neighbour sensors, due to the high transmission of mechanical stimulus through the polymer.[2]

To overcome these drawbacks, research is increasing towards polymer geometries where the active part of the tactile sensor is lifted up from the substrate surface forming three dimensional structures such as pyramids,[2] bumps and domes.[19] These structures have several advantages: reduction of sensors' cross-talk, broadening of sensors' sensitivity to small forces and very high effectiveness during grasping actions. The fabrication of these structures usually requires additional steps that increase the complexity of the process, consequentially affecting the final yield.

Here we study an AlN semiconductor material deposited on a polymeric substrate which manifests a natural organization of a

[a]*Center for Biomolecular Nanotechnologies@UniLe, Istituto Italiano di Tecnologia, Via Barsanti, 73010 Arnesano (LE), Italy. E-mail: simona.petroni@iit.it; Fax: +39 0832 295708; Tel: +39 0832 295726*
[b]*Nanophysics, Istituto Italiano di Tecnologia, via Morego, 30, 16163 Genova, Italy. E-mail: bruno.torre@iit.it; Fax: +39 010 7170187; Tel: +39 010 71781*
[c]*National Nanotechnology Laboratory Istituto Nanoscienze – CNR, Via Arnesano, 73100 Lecce, Italy. E-mail: mariateresa.todaro@unisalento.it; Fax: +39 0832 298386; Tel: +39 0832 298373*
[d]*Dip. di Ingegneria dell'Innovazione, Università del Salento, Via Arnesano, 73100 Lecce, Italy. E-mail: massimo.devittorio@unisalento.it; Fax: +39 0832 298386; Tel: +39 0832 298200*

circular capacitor in a dome shape, due to the compressive stress of the AlN over the polymer. Moreover the material shows a moderate capacitive response ascribed to the strain gradient generated into the layer under uniform stress, known as the flexoelectric effect.[20] AlN is a dielectric material presenting interesting electrical properties: natural piezoelectricity due to the crystal symmetry C_{6v}, retained as long as the crystal is stable (up to 1500 °C), piezoelectric coefficient d_{33} of 4–5 pC N^{-1},[21] wide energy band gap of 6.2 eV, high electrical resistance, high breakdown voltage and low dielectric loss. The lack of flexibility and conformability of AlN has already been dealt with in some previous works by Akyiama *et al.*,[22] through sputtering deposition of AlN on polyimide at room temperature. The integration of piezoelectric AlN on organic soft materials results in an extremely efficient technology, combining the electronic/piezoelectric properties of inorganic semiconductors with the mechanical properties of polymers.[23]

In this work we present flexible tactile sensors based on AlN of high crystal quality, realized by using moderate temperature reactive sputtering on a large area polymeric and flexible film of kapton HN. AlN piezoelectric layers are embedded in molybdenum electrodes on kapton substrates. The (Mo)/AlN/Mo/Kapton multi-layered structure presents both piezoelectric and flexoelectric transduction mechanisms. Recently, multisensing approaches have been emerging[24] as the most promising ones to improve the efficiency and reduce the complexity of artificial sensing systems. Here, the coexistence of two transduction mechanisms is realised by the same technology, allowing us to detect both static and dynamic stimuli through flexoelectric and piezoelectric effects, respectively. Moreover, it is worth mentioning that, to our knowledge, the exploitation of flexoelectricity in AlN for sensing applications is presented here for the first time.

Experimental

The samples are prepared by laminating the kapton HN tape on a silicon support. The tape, composed of 25 μm of kapton and 60 μm of silicone adhesive, will constitute the flexible substrate of the tactile sensors. After a standard cleaning of the substrate with IPA, acetone and DI water, the structure composed of a bottom electrode of Mo (120 nm), a piezoelectric layer of AlN (700 nm) and a top electrode of Mo is deposited by DC sputtering. The difference in the Young modulus of AlN (389 GPa) and kapton (2.5 GPa)[25] enhances the static bulk flexoelectricity as described by Tagantsev.[26]

Flexible AlN synthesis

The deposition of inorganic layers on polymers usually presents some challenges related to the temperature that the organic material can sustain. This limit forces the synthesis to be performed at room temperature, whilst the crystal quality of the inorganic layer is improved by depositions at high temperature. Therefore the Mo/AlN/Mo structure is grown by a LLSEVO magnetron sputtering system, increasing the temperature of the process chamber during AlN deposition. The layers are deposited by DC sputtering in a single run with the following process parameters. The Mo layer is deposited from a high-purity (99.999%) Mo target at room temperature, with a total pressure of 1.5×10^{-3} mbar in Ar atmosphere and a DC power of 500 W. The AlN layer is grown, after heating the process chamber up to 70 °C, with a gas mixture of N_2 (14.5 sccm) and Ar (10 sccm) at a pressure of 1.2×10^{-3} mbar. The DC power is 2250 W and a bias voltage of −50 V is applied to the sample holder to enhance the energy of the plasma. The chamber temperature rises to 250–300 °C during the reactive sputtering process, which is compatible with the kapton film.[25] The topmost Mo layer is deposited after cooling down the chamber and under the same conditions reported above.

X-ray diffraction spectra

The sample is observed with a FEI NOVA NanoSEM 200 and the crystal structure and crystalline state of the films examined using X-ray diffraction (XRD) on an X'Pert PRO MRD Panalytical diffractometer operating in the Bragg-Brentano geometry using Cu-Kα1 radiation at $\lambda = 1.5418$ Å. The diffracted intensities are collected in the θ–2θ scan mode in the range 5°, 2θ, 120° with a step size of 0.01°. The crystal orientation was evaluated from the full width at half-maximum (FWHM) of X-ray rocking curves.

High resolution TEM

High Resolution TEM (HRTEM) analysis is carried out by a Jeol 2200FS microscope with a spherical aberration-corrected objective lens, equipped with a Field Emission Gun (FEG) and working at an acceleration voltage of 200 kV. The HRTEM images are recorded by a Gatan Ultrascan 1000 CCD camera. The structural features of the nanostructures images are studied by Fourier analysis of the 2D-Fast Fourier Transform of the HRTEM images.

Atomic force microscopy d_{33} characterization

The piezoelectric constant d_{33} is measured through a direct evaluation of the strain generated when the electric field is applied (converse piezoelectric effect). The off-plane deformation has been detected by using an Atomic Force Microscope (Asylum Research, MFP-3D) in point mode, measuring the cantilever deflection at reduced feedback loop gain to compensate for thermal drifts. Large area sensors ending with polystyrene micrometric beads (61.7 ± 0.1 μm diameter beads, Polyscience, Inc) mounted on the silicon tipless cantilever (Nanoworld), have been developed to enhance accuracy, to reduce boundary effects (*i.e.* in plane spurious deformations) and tip induced deformations.[27]

Capacitance characterization

The capacitive response is demonstrated on circular parallel plate capacitors realized by a single photolithographic process. The capacitors, after the dry etching of the top Mo/AlN layers, take a dome shape due to the partial release of residual stress of the crystal layers on Mo and flexible kapton. These structures are very elastic and deformable and their conformability is assessed after a bending cycle on cylindrical shapes with different radii of curvature. Thereby, AlN is not only studied for its piezoelectric

response, already exhaustively analyzed in previous works,[28–32] but for its significant capacitance variation under uniform normal stress, which generates a strain gradient in the crystal texture. The capacitance measurements are performed by an Agilent E4980A Precision LCR meter at a frequency of 1 kHz and by applying a voltage of 4 V. The capacitance is measured in the parallel equivalent circuit mode, which is recommended when capacitance is small (around 130 pF). The Q factor provided by the instrument during C_p measurement is proportional to the reactance of the DUT (device under testing) through the formula: $Q = |X|/R$ and in general it is high for small capacitances. Q is the parameter used to test the functional integrity of the device after bending.

Results and discussion

Among available deposition techniques,[33,34] reactive sputtering is characterized by good crystal quality at moderate deposition temperature, which is compatible with CMOS technologies and with some organic substrates.[23] The structure and crystalline state of the film are analyzed by X-ray diffraction (XRD). The diffracted intensities collected in the θ–2θ scan mode in the range 5°, 2θ, 120° (Fig. 1a) show the AlN peak, less intense than Mo, at about 36° for the reflection (0002) corresponding to the AlN hexagonal structure. Mo exhibits a strong peak at 2θ at about 41° due to the reflection (110) while a second weak peak for the reflection (211) is at approximately $2\theta \approx 74°$. The rocking curve of the AlN (0002) shown in Fig. 1b has a full width at half maximum (FWHM) of 0.55° (Fig. 1b). The narrow peak of the rocking curve indicates a high orientation of the polycrystalline material obtained by sputtering. The value 0.55° is as good as values reported for well oriented AlN grown by sputtering on silicon substrates.[35]

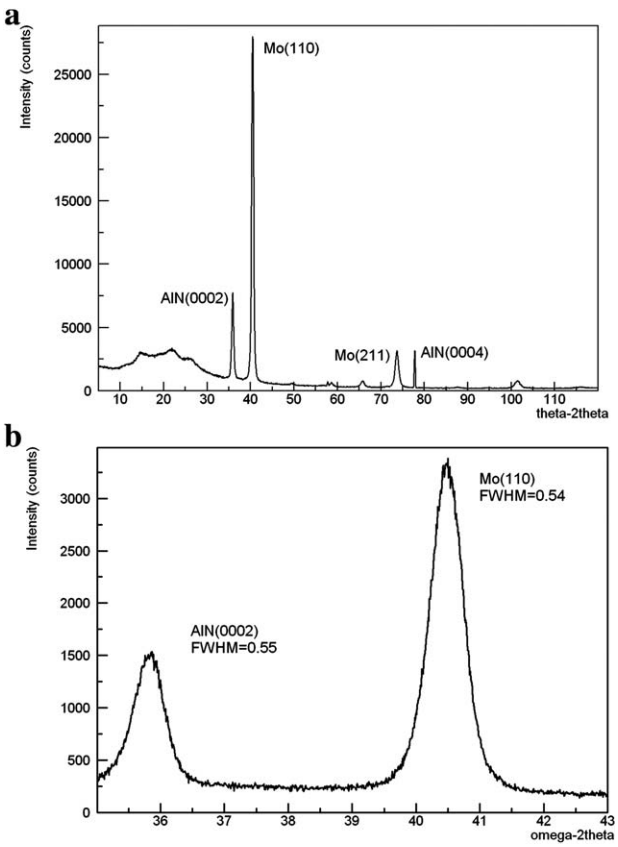

Fig. 1 (a) X-Ray diffraction spectra θ–2θ with $5° < \theta > 120°$ for the structure Mo(120 nm)/AlN(700 nm)/Mo(120 nm); (b) rocking curve of the AlN (0002) peak has a full width at half maximum (FWHM) of 0.55.

The material is further investigated by transmission electron microscopy to assess that the c-axis is perpendicular to the substrate. Low and high-magnification HRTEM pictures in Fig. 2a and b show the central layer in a polycrystalline hexagonal structure with columnar arrangement, where each column perpendicular to the substrate is constituted by a single crystal.

Thereafter the electrical characterization of the material is performed on parallel plate capacitors realized by one lithographic step. After the deposition, the sample is masked with SU8-25 negative resist to define the top electrode and the AlN layer in a single etching step. The dry etching is performed by an ICP (Inductively Coupled Plasma) based on the gas mixture $SiCl_4$, N_2 and Ar. The kapton sample is then peeled off from the rigid support of silicon, dipping the sample into hot iso-propanol (120 °C) for 1 h. The silicone adhesive used to grip the sample to silicon results to be very important during the sputtering deposition and dry etching to dissipate thermal energy. Trials on floating foils have shown a modification of kapton elastic properties during ICP etching.

The dry etching engraves in a single step that the top electrode and the AlN layer with the same geometry and the Mo bottom electrode forms a continuous layer for a common electrical ground. The circular parts of the transducers adopt a typical dome shape, as shown in Fig. 3a and b. The compressive residual stress of the Mo and AlN crystal layers produces an evident bowing of the polymer that in some areas interrupts the common ground metal layer as shown by SEM images in Fig. 3c and d.

The piezoelectricity of the synthesized AlN is assessed by measuring the AlN piezoelectric constant d_{33} by AFM piezo response through a direct evaluation of the strain when the electric field is applied. The off-plane deformation has been detected by using an Atomic Force Microscope in point mode measuring the cantilever deflection. The measured piezoelectric coefficient on the sample at 5 V is $d_{33} = 4.7 \pm 0.5$ pm V^{-1}, which is consistent with the value reported for AlN layers grown on silicon and silicon-based substrates.[21]

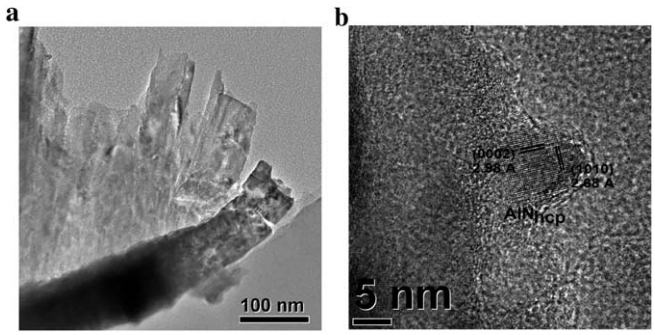

Fig. 2 High resolution TEM shows hexagonal crystal structure with a c-axis perpendicular to the substrate where each column is represented by a monocrystal.

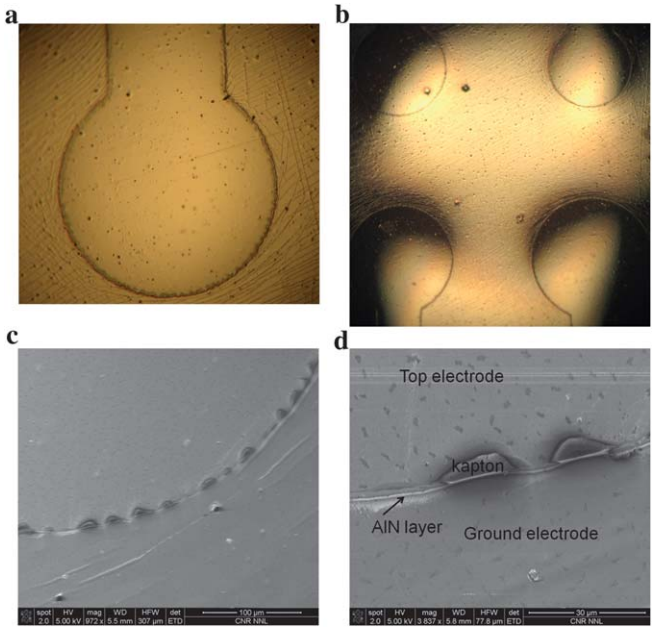

Fig. 3 (a) Parallel plate capacitor dome with a diameter of 600 μm. (b) Section of a set of sensors with different diameters from 500 μm to 800 μm. (c) SEM image of the capacitor. (d) SEM image of the material interfaces.

The piezoelectricity of AlN on polyimide has already been studied on the unstructured material by Akiyama *et al.* in ref. 22 as an efficient transduction mechanism of dynamic forces.

We report on the flexoelectric effect of bowed parallel plate capacitors generated by the dissimilar elastic properties of the AlN and polyimide. The flexoelectric effect is the ability of piezoelectric (and dielectric) materials to generate charge separation when subjected to elastic strain gradients.[20] The polarization is described by the formula:

$$P_l = \mu_{ijkl} \frac{\partial S_{ij}}{\partial x_k} \quad (1)$$

where P_l is the resultant polarization, μ_{ijkl} the flexoelectric coefficients, S_{ij} the components of the elastic strain, and x_k the direction of the strain (S) gradient.

The static and dynamic characteristics of polarization have been studied by Tagantsev; he defines the static contribution to the polarization as due to the discontinuity of the crystal lattice.[26] We experimentally observed this polarization effect as a capacitance variation ΔC when a load is applied over the dome. During the load application, the AlN layer experiences in plane strain which changes across the dome section.

The capacitance variation ΔC is measured as a function of the pressure (Fig. 4), calculated applying loads from 1 g (~0.01 N) to 20 g (~0.2 N). The loads are applied on the circular part of the transducer, which has diameters from 500 to 800 μm. The sensitivity increases with the diameter of the structure up to a maximum of 4×10^{-3} pF kPa^{-1}. The dielectric constant ε of AlN, measured from the fabricated parallel plate capacitors, is 8.2 ± 0.5 at 1 kHz, which is consistent with the value reported in previous work.[36]

This flexoelectric effect of flexible AlN on polyimide improves the sensing performances of this material, which can be used

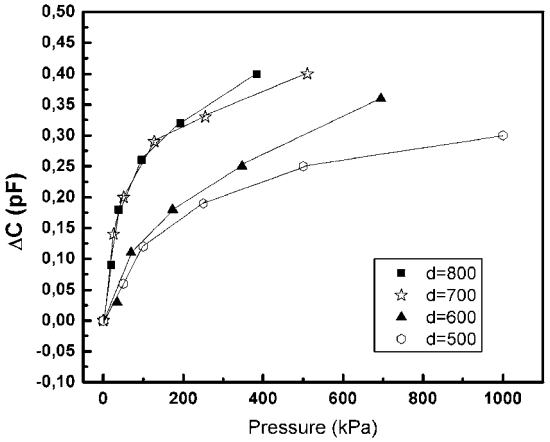

Fig. 4 Capacitance change DC of sensors with different diameters 500, 600, 700, 800 by applying loads of 1, 2, 5, 10, and 20 g.

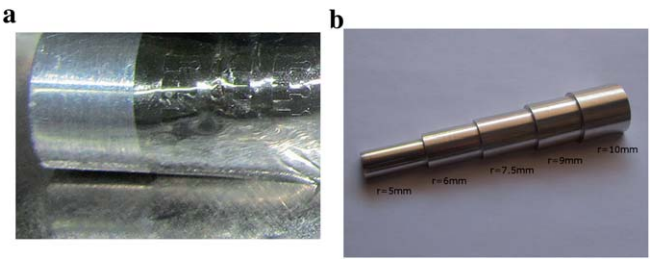

Fig. 5 Flexibility test. (a) Sample under bending cycle; (a) curved surface of radius 5, 6, 7.5, 9, and 10 mm on which the sensing foil is bent.

either for dynamic and static forces of small and medium intensity.

The dome transducers presented in this work are very elastic and the deformations of the substrate seem to not affect the electrical performances of the devices. In order to assess flexibility, feasibility and preservation of electrical performances of the device after bending stress, we have monitored its Q factor and capacitance before and after the deformation[37] of the sensing foil on curved surfaces (Fig. 5a) of different curvature radii from 10 mm to 5 mm, comparable to the dimensions of the human finger. The capacitance and Q factor are measured after bending cycles of 1 hour. The capacitance shift is within ± 0.04 pF and the average quality factor (Q) remains as high as 210. Preliminary measurements on the durability of the devices have been performed by applying tens of deformation cycles without noticing any effect on the sensor response.

Conclusions

In summary AlN of high crystal quality, comparable to what is typically achieved on silicon,[34] is integrated on a polymeric substrate such as kapton. Circular parallel plate capacitors fabricated on the flexible substrate take a typical dome shape due to the compressive stress of AlN on kapton. The dome shows a significant capacitive variation under normal forces in static mode in the range of interest for tactile sensing applications. This static capacitive response is ascribed to the flexoelectric effect, which is the ability to generate a charge separation when a strain

gradient is present in the material. The presented sensors have the fundamental requirements for robotic applications such as sensitivity to a gentle touch, sensing on a large area, and moderate sensitivity to applied pressure $(4 \times 10^{-3}$ pF kPa$^{-1})^2$ in a wide pressure range from 10 kPa to 1 MPa. This technology could potentially solve the issue of sensors' density on artificial skin, exploiting the same material and architecture for the detection of static and dynamic stimuli as it occurs in human receptors. Moreover being that these properties are due to the residual stress on kapton of thin polycrystalline layers deposited by sputtering, the mechanical properties of the sensors can be easily modified through deposition parameters and different buffer layers.

Acknowledgements

The authors would like to acknowledge technicians Mario Malerba, Diego Mangiullo and GianMichele Epifani for their helpful support. This research has been supported by Italy–Japan FIRB HUB on Nanotechnologies.

References

1 J. A. Carlson, J. M. English and D. J. Coe, *Smart Mater. Struct.*, 2006, **15**, N129.
2 S. C. Mannsfeld, B. C.-K. Tee, R. M. Stoltenberg, C. V. Chen, S. Barman, B. Muir, A. N. Sokolov, C. Reese and Z. Bao, *Nature*, 2010, **9**, 859–864.
3 N. Bu, O. Fukuda, N. Ueno and M. Inoue, *IEEE Proceedings International Conference on Robotics and Biomimetics*, 2009, pp. 944–948.
4 A. W. Lees, *J. Phys.: Conf. Ser.*, 2009, **181**, 012019.
5 Y. Qi, N. T. Jafferis, K. Lyons, C. M. Lee, H. Ahmad and M. C. McAlpine, *Nano Lett.*, 2010, **10**, 524–528.
6 R. S. Dahiya, G. Metta, M. Valle and G. Sandini, *IEEE Trans. Robot.*, 2010, **26**, 1–20.
7 M. E. H. Eltaib and J. R. Hewit, *Mechatronics*, 2003, **13**(10), 1163–1177.
8 J. Dargahi and M. Parameswaran, *J. Microelectromech. Syst.*, 2000, **9**, 329–335.
9 J. Engel, N. Chen, C. Tucker, C. Liu, S.-H. Kim and D. Jones, in *IEEE Conference on Sensors*, Daegu, Korea, 2006, pp. 563–566.
10 M. Y. Cheng, X. H. Huang, C. W. Ma and Y. J. Yang, *J. Micromech. Microeng.*, 2009, **19**, 115001.
11 Y. Ohmura and H. Kuniyoshi, in *IEEE/RSJ International Conference on Intelligent Robots and Systems*, San Diego, CA, USA, 2007.
12 H. Shinoda, K. Matsumoto and S. Ando, *Transducer'97, Chicago, In Conference on, Solid State Sensors and Actuators*, 1997, vol. 1, pp. 129–137.
13 M. Goka, H. Nakamoto and S. Takenawa, *IEEE/RSJ Int. Conference on Intelligent Robots and Systems (IROS)*, 2010, pp. 885–890.
14 S. Nambiar and J. T. W. Yeow, *Biosens. Bioelectron.*, 2011, **26**(5), 1825–1832.
15 N. Wettels, V. J. Santos, R. S. Johansson and G. B. Loeb, *Adv. Robot.*, 2008, **22**(12), 829–849.
16 P. Dario, D. De Rossi, C. Dornenici and R. Francesconi, in *Proc. 1st IEEE Int. Conf. on Robotics*, 1984, pp. 332–340.
17 E. S. Kolesar, C. S. Dyson, R. R. Reston, R. C. Fitch, D. G. Ford and S. D. Nelms, *Innovative Systems in Silicon, 1996, Proceedings, Eighth Annual IEEE International Conference on*, 1996, pp. 372–381.
18 A. M. Vinogradov, V. H. Schmidt, G. F. Tuthill and G. W. Bohannan, *Mech. Mater.*, 2004, **36**, 1007–1016.
19 C. Li, P.-M. Wu, S. Lee, A. Gorton, M. J. Schulz and C. H. Ahn, *J. Microelectromech. Syst.*, 2008, **17**(2), 334–341.
20 L. E. Cross, *J. Mater. Sci.*, 2006, **41**, 53–63.
21 A. Ababneha, U. Schmidb, J. Hernandoc, J. L. Sánchez-Rojasc and H. Seidela, *Mater. Sci. Eng., B*, 2010, **172**, 253–258.
22 M. Akiyama, Y. Morofuji, T. Kamohara, K. Nishikubo, Y. Ooishi, M. Tsubai, O. Fukuda and N. Ueno, *Adv. Funct. Mater.*, 2007, **17**, 458–462.
23 M. Akiyama, Y. Morofuji, K. Nishikubo and T. Kamohara, *Appl. Phys. Lett.*, 2008, **92**, 043509.
24 C. Pang, G.-Y. Lee, T. Kim, S. M. Kim, H. N. Kim, S.-H. Ahn and K.-Y. Suh, *Nat. Mater.*, 2012, **11**, 795–801.
25 www2.dupont.com/Kapton.
26 A. K. Tagantsev, *Phys. Rev. B: Condens. Matter Mater. Phys.*, 1986, **34**(8), 5883.
27 R. S. Dahiya, B. Torre, R. Cingolani and G. Sandini, *IEEE Proc. Nanotechnology*, 2009, pp. 670–673.
28 M. Akiyama, Y. Morofuji, T. Kamohara, K. Nishikubo, M. Tsubai, O. Fukuda and N. Ueno, *J. Appl. Phys.*, 2006, **100**, 114318.
29 T. Kobayashi, H. Okada, M. Akiyama, R. Maeda and T. Itoh, *Solid-State Sensors, Actuators and Microsystems International Conference*, 2009, pp. 1166–1169.
30 M. Tsubai, N. Ueno, O. Fukuda and M. Akiyama, *International Joint Conference SICE-ICASE*, 2006, pp. 3827–3830.
31 S. Petroni, G. Maruccio, F. Guido, M. Amato, A. Campa, A. Passaseo, M. T. Todaro and M. De Vittorio, Flexible piezoelectric cantilevers fabricated on polyimide substrate, *Microelectron. Eng.*, 2012, **98**, 603–606.
32 S. Petroni, C. La Tegola, G. Caretto, A. Campa, A. Passaseo, M. De Vittorio and R. Cingolani, *Microelectron. Eng.*, 2011, **88**(8), 2372–2375.
33 Z. Chen, S. Newman, D. Brown, R. Chung, S. Keller, U. K. Mishra, S. P. Denbaars and S. Nakamura, *Appl. Phys. Lett.*, 2008, **93**, 191906.
34 S. S. Hullavarad, R. D. Vispute, B. Nagaraj, V. N. Kulkarni, S. Dhar, T. Venkatesan, K. A. Jones, M. Derenge, T. Zheleva, M. H. Ervin, A. Lelis, C. J. Scozzie, D. Habersat, A. E. Wickenden, L. J. Currano and M. Dubey, *J. Electron. Mater.*, 2006, **35**(4), 777–794.
35 F. Martin, P. Muralt, M. A. Dubois and A. Pezous, *J. Vac. Sci. Technol., A*, 2004, **22**, 361–365.
36 J. M. Wagner and F. Bechstedt, *Phys. Rev. B: Condens. Matter Mater. Phys.*, 2000, **62**(7), 4526–4534.
37 K. Song, J. Noh, T. Jun, Y. Jung, H.-Y. Kang and J. Moon, *Adv. Mater.*, 2010, **22**, 4308–4312.

